HHS Public Access

Author manuscript

Cell Rep. Author manuscript; available in PMC 2022 November 14.

Published in final edited form as:

Cell Rep. 2022 October 25; 41(4): 111534. doi:10.1016/j.celrep.2022.111534.

The locus coeruleus mediates behavioral flexibility

Jim McBurney-Lin[1,2,4], **Greta Vargova**[1,4], **Machhindra Garad**[1], **Edward Zagha**[2,3], **Hongdian Yang**[1,2,5,*]

[1]Department of Molecular, Cell and Systems Biology, University of California, Riverside, Riverside, CA 92521, USA

[2]Neuroscience Graduate Program, University of California, Riverside, Riverside, CA 92521, USA

[3]Department of Psychology, University of California, Riverside, Riverside, CA 92521, USA

[4]These authors contributed equally

[5]Lead contact

SUMMARY

Behavioral flexibility is the ability to adjust behavioral strategies in response to changing environmental contingencies. A major hypothesis in the field posits that the activity of neurons in the locus coeruleus (LC) plays an important role in mediating behavioral flexibility. To test this hypothesis, we developed a tactile-based rule-shift detection task in which mice responded to left and right whisker deflections in a context-dependent manner and exhibited varying degrees of switching behavior. Recording spiking activity from optogenetically tagged neurons in the LC at millisecond precision during task performance revealed a prominent graded correlation between baseline LC activity and behavioral flexibility, where higher baseline activity following a rule change was associated with faster behavioral switching to the new rule. Increasing baseline LC activity with optogenetic activation accelerated task switching and improved task performance. Overall, our study provides important evidence to reveal the link between LC activity and behavioral flexibility.

In brief

McBurney-Lin and Vargova et al. measure spiking activity from neurons in the locus coeruleus (LC) during a tactile-based rule-shift task to test the role of LC in behavioral flexibility. LC baseline activity exhibits a prominent correlation with the speed of rule switching. Increasing LC baseline activity facilitates behavioral switching.

*Correspondence: hongdian@ucr.edu.

AUTHOR CONTRIBUTIONS

J.M.-L. and H.Y. planned the project and built the apparatus. J.M.-L. performed experiments with assistance from M.G. J.M.-L., G.V., and H.Y. analyzed data and wrote the manuscript with inputs from M.G. and E.Z.

DECLARATION OF INTERESTS

The authors declare no competing interests.

SUPPLEMENTAL INFORMATION

Supplemental information can be found online at https://doi.org/10.1016/j.celrep.2022.111534.

Graphical Abstract

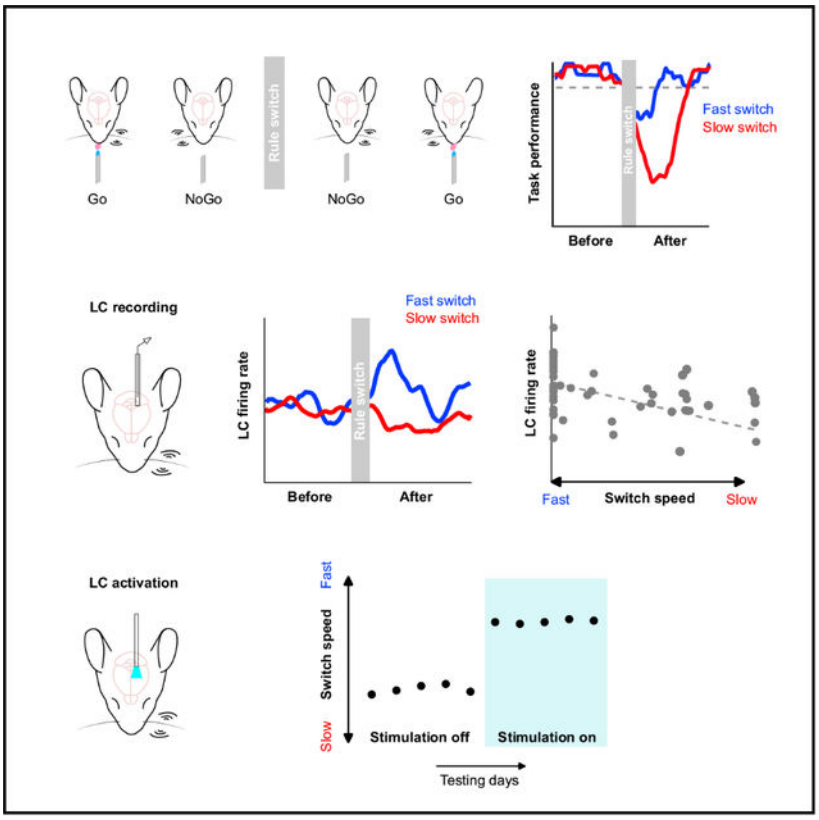

INTRODUCTION

Behavioral flexibility, the ability to adapt goal-directed responses to changing environmental contexts and demands, is critical to the survival of organisms. For example, a pedestrian in New York should first look left to check oncoming traffic before crossing a street. The same person in London would suppress this habitual response and look to the right instead. Inappropriate behavioral adaptations are observed in a broad spectrum of psychiatric disorders and aging (Uddin, 2021). Understanding the neural substrates of behavioral flexibility is a major topic of systems neuroscience research.

Several key brain structures have been implicated in supporting flexible behavioral switching (e.g., Bartolo and Averbeck, 2020; Birrell and Brown, 2000; Cope et al., 2019; Devauges and Sara, 1990; Durstewitz et al., 2010; Glennon et al., 2019; Janitzky et al., 2015; Lapiz and Morilak, 2006; Martins and Froemke, 2015; Rich and Shapiro, 2009; Tervo et al., 2014), including the noradrenergic nucleus locus coeruleus (LC). A major hypothesis in the field posits that the activity of LC neurons plays a critical role in mediating behavioral flexibility (Aston-Jones and Cohen, 2005; Aston-Jones et al., 1999; Sara and Bouret, 2012). This hypothesis is primarily built upon electrophysiological evidence from non-human primates and rodents that LC responds to salient stimuli and that LC activity reflects behavioral states and task performance (e.g., Aston-Jones and Bloom, 1981; Aston-

Jones et al., 1994; Clayton et al., 2004; Rajkowski et al., 1994, 2004; Usher et al., 1999). Other recording and perturbation studies have further suggested a link between LC and exploratory behavior (Kane et al., 2017; Koralek and Costa, 2021) or a link between LC and rule change-related behavior (Aston-Jones et al., 1997; Bouret and Sara, 2004; Glennon et al., 2019; Janitzky et al., 2015; Xiang et al., 2019). However, it is still unclear whether and how LC activity (more specifically, the type of LC activity) is linked to different degrees of behavioral flexibility in a graded manner and whether and how perturbing the LC causally affects rapid behavioral switching to the new rule during a well-controlled, quantitative flexibility task. Answering these questions is a critical step toward unraveling the molecular, cellular and circuit mechanisms underlying LC modulation of behavioral flexibility and cognitive functions.

To begin to bridge these knowledge gaps and to assess the extent to which the LC contributes to flexible behavioral switching, we developed a tactile-based rule-shift detection task in head-fixed mice, in which mice were trained to respond to left and right single-whisker deflections in a context-dependent manner and exhibited varying degrees of switching behavior within individual sessions. During task performance, we recorded spiking activity from optogenetically tagged noradrenergic neurons in the LC at millisecond precision and established a graded relationship between LC spiking activity and the degree of flexible task switching. Higher behavioral flexibility (faster switching to the new rule) was characterized by a greater increase in baseline LC activity upon the rule change, whereas lower behavioral flexibility (slower switching to the new rule) was characterized by a reduced baseline activity. Increasing baseline LC activity with optogenetics led to robust improvements in task switching and task performance. Together, our data provide important evidence to reveal the link between LC activity and behavioral flexibility.

RESULTS

We developed a tactile-based rule-shift detection task to probe behavioral flexibility in mice, following the concepts from recent task designs in head-fixed rodents (Banerjee et al., 2020; Chevée et al., 2021; Glennon et al., 2019; Reinert et al., 2021). There were two rules in the task, Left Go and Right Go, and mice were trained to adapt to repeated rule changes within individual behavioral sessions (Figures 1A–1C; STAR Methods). On each trial, one of the two whiskers (left or right C2) was stimulated. For the Left Go rule, left whisker deflection was the Go stimulus and right whisker deflection was the NoGo stimulus, and vice versa for the Right Go rule. Licking during a response window following whisker stimulation determined trial outcome (Figures 1B and 1C). Individual sessions typically consisted of 2 or 3 blocks (i.e., 1 or 2 rule switches), with each block consisting of 100–200 trials. The rule of the first block (block 1) was randomly assigned, and each subsequent block had the alternate rule as the preceding block (e.g., block 1, Left Go; block 2, Right Go; Figure 1A). The beginning of each block consisted of 5–10 “cueing trials,” in which the presentation of the Go stimulus was paired with water delivery (STAR Methods). As block 1 did not involve a rule change, subsequent analyses were focused on the blocks following block 1, with switch performance defined as task performance (fraction correct) in these blocks. The training process took several weeks (Figures S1A, S1B, and 1D; STAR Methods), and mice were considered trained once their switch performance in block 2 was above 65% for two

consecutive days (Chevée et al., 2021). The learning progression appeared to be associated with an increase of correct rejection rate, rather than hit rate (Figure 1D). Mice were able to perform Left Go and Right Go blocks at similar levels (i.e., no apparent "handedness"; Figure S1C), so both types of blocks were pooled in subsequent analyses.

Overall, task performance decreased upon the rule change because of the drop of both hit rate and correct rejection rate. After the rule change, performance tended to recover slowly, indicating that mice progressively adapted to the new rule (Figure S1D). We noticed that trained mice exhibited varying levels of switching behavior following the rule change (Figure 1E). To quantify the degree of flexible task switching, we defined a behavioral switch point where task performance in a 50 trial moving window surpassed a threshold of 85% (Figure 1E). According to the definition (STAR Methods), a switch point of 1 trial meant that task performance surpassed the threshold during the first 50 trial window, and it did not necessarily mean that the mouse already switched to the new rule on trial 1. Intuitively, behavioral switch point exhibited a strong negative correlation with switch performance (Figure 1F). As behavioral switch point followed a bimodal distribution separated around trial 50, we referred to blocks with switch point below trial 50 as "fast switch" blocks (more flexible) and those above as "slow switch" blocks (less flexible; Figure 1G). As expected, switch performance in fast blocks was higher than in slow blocks (Figure 1H). To test whether such differences in switch performance were due to variations in motivational states (Allen et al., 2019; Berditchevskaia et al., 2016; McBurney-Lin et al., 2020), we conducted further analysis to show that neither fast nor slow blocks were preferentially concentrated toward the beginning or the end of individual sessions (Figure S1E). Additionally, reaction time and number of licks were not different between fast and slow blocks (Figure S1F). These results suggest that motivational changes during a session cannot account for the differences in task switching between fast and slow blocks. Together, our data demonstrate that mice exhibited varying degrees of switching behavior in the novel rule-shift detection task.

Next, we recorded spiking activity from optogenetically tagged single neurons in the LC along with pupil diameter during task performance (Figures 2A–2C; STAR Methods). On the basis of previous work (Aston-Jones and Cohen, 2005; Aston-Jones et al., 1997; Usher et al., 1999; Yang et al., 2021), we hypothesized that the pre-stimulus baseline LC activity was associated with the degree of behavioral flexibility. To test this, we first analyzed baseline LC activity (quantified in a 1 s window prior to whisker stimulation onset) before and after the rule change in a subset of sessions where a fast switch block and a slow switch block both occurred (14 blocks of 7 sessions from 3 mice, for paired comparison; 1 fast block and 1 slow block per session, 1 single-unit recording per session; STAR Methods) and found that LC spiking was transiently elevated following the rule change only in the fast switch blocks (Figures 2D–2F). That is, in blocks in which mice more rapidly adapted their responses to the new rule, baseline LC activity was transiently elevated following the rule change (after), compared with baseline activity right before the rule change (i.e., at the end of the previous block: before; Figures 2E–2G; STAR Methods). The changes in baseline activity upon the rule shift (Δ firing rate = after − before) were also higher in fast blocks than slow blocks (fast versus slow, 0.50 ± 0.16 versus -0.28 ± 0.16 spikes/s; $p = 0.002$; Figure 2H). Similar trends held when we included additional fast and slow blocks that were not from

the same sessions (unpaired comparison, 49 blocks of 34 sessions from 6 mice; Figure S2A; 1 single-unit recording per session). Importantly, independent from categorizing switching behavior into fast and slow, the changes in baseline LC activity exhibited a prominent negative correlation with behavioral switch point (Figure 2I). The same relationship held when baseline LC activity was quantified in different time windows (Figures 2J and S3). This relationship also held in the great majority of cases when we varied trial window size and performance threshold to determine behavioral switch point (Table S1), strengthening the link between LC activity and different levels of behavioral flexibility. We also note that varying these parameters to determine behavioral switch point could potentially reduce the ceiling effect of switch point of 1 trial and better grasp the variability in switching behavior of these mice (Figure S2B). Licking behavior during fast and slow switch blocks were similar (Figure S2C), and the relationship between LC activity associated with fast and slow switches was robust when we only included hit trials in the analysis (Figure S2D). In addition, baseline activity was quantified prior to any possible licking events in a trial. Together, these lines of evidence suggest that the observed changes in LC activity were not a direct effect of licking itself (Zagha et al., 2022).

To further determine whether the changes in baseline LC activity reflected true differences in behavioral flexibility, we quantified task performance in trial blocks immediately preceding the identified fast and slow switch blocks. Performance in blocks immediately preceding the fast blocks (i.e., blocks with the opposite rule) was comparable with the performance in those fast blocks. In contrast, task performance in blocks immediately preceding the slow blocks was higher than the performance in the slow blocks (Figure S2E). These results suggest that (1) the identified fast switch blocks and the associated LC activity reflected true enhanced flexible task switching, such that mice were adapting to both rules, instead of simply following one rule, and (2) the identified slow switch blocks and the associated LC activity reflected true reduced ability to switch to the new rule, rather than an overall lack of performance/engagement in the session. Although pupil diameter was bigger in the after period in both types of switches, the changes in pupil diameter upon the rule shift (Δ pupil = after − before) were slightly bigger in the fast switch blocks (Figure S2F), demonstrating similarities and differences in the relationship between behavior and LC activity/pupil diameter (Megemont et al., 2022). Overall, our data indicate that baseline LC activity was prominently correlated with different degrees of flexible task switching, such that higher baseline activity following the rule change was associated with a faster behavioral adaptation to the new rule (more flexible). In contrast, lower baseline activity was associated with a slower behavioral switch (less flexible).

Next, to determine the causal role of LC activity in task switching (sufficiency), we optogenetically activated LC neurons during behavior. We noticed that LC activity exhibited considerable session-to-session fluctuations in both fast and slow switches during the “before” period, such that both switches could be associated with a wide range of baseline firing rate before the rule change, sometimes as high as 2–5 spikes/s and occasionally even higher than 5 spikes/s (Figures 2G and S2A). Thus, we wanted to use a stimulation strength that was safely above this “noisy” range of baseline activity, which would have a higher likelihood to induce a measurable behavioral effect. Adapting from a previous paradigm (Glennon et al., 2019), we stimulated LC at 10 Hz in a 0.5 s window prior to whisker

stimulation onset in trials following the rule change (Figure 3A; STAR Methods), the same time window in which the graded relationship between baseline LC activity and the degree of task switching was established (Figure 2J). Stimulating LC at this high-tonic range was also meant to compensate the limiting factor that optical stimulation only drove a subset of neurons. We recruited mice that had been trained for an extended period (>4 weeks) with switch performance consistently below the 65% threshold. Therefore, these mice were considered over-trained poor performers. Mice were placed in the test and control group after histological examination of optical fiber placement. Therefore, channelrhodopsin-2 (ChR2) was expressed in the LC of both test and control groups, but test group had the optic fiber targeted the LC, and the control group had the optic fiber off-targeted the LC (i.e., LC was not stimulated or was minimally stimulated by blue light; Figures 3A and S4A). Confirmation of fiber implant was assisted by the presence/absence of pupil response to optical stimulation (Figures 3B and S4B; Megemont et al., 2022; Privitera et al., 2020). Compared with previous sessions without stimulation (baseline), switch performance of the test group noticeably improved upon LC stimulation (Figures 3C, 3F, and S4C; baseline versus stimulation, 0.52 ± 0.02 versus 0.69 ± 0.02 fraction correct; $p = 1.6e\text{-}5$), and the improvement was present in individual mice (Figures 3D and S4D). The behavioral effects were specific to the switching blocks, as performance in the first block (block 1, no rule shift) was not affected (Figure S4E), suggesting that our LC stimulation protocol did not evoke nonspecific effects. LC stimulation also accelerated task switching in the test group (behavioral switch point, baseline versus stimulation, 154 ± 8 versus 116 ± 13 trials; $p = 0.02$; Figure 3G). As a result, activating LC appeared to “rescue” the switching behavior of these over-trained but poorly performing mice. LC activation increased correct rejection rate, but not hit rate (Figures 3H, 3I, and S4F), in line with a previous report (Glennon et al., 2019) as well as the learning progression (Figure 1D). In contrast, optical stimulation had no effects on task switching in the control group (Figures 3C and 3E–3G; Figures S4C, S4D, and S4G). The behavioral effects between test and control groups were robust when the comparisons were made across mice (Figure S4H). Licking behavior was not influenced by optical stimulation (Figures S4I and S4J) and thus cannot account for the improved correct rejection rate, further suggesting that this stimulation protocol did not evoke nonspecific effects. In summary, increasing baseline LC activity facilitated switching to the new rule.

DISCUSSION

In this work, we set out to test the hypothesis that the LC is involved in mediating behavioral flexibility. We developed a tactile-based rule-shift detection task in which head-fixed mice exhibited varying degrees of flexible task switching upon a rule change within single sessions. Using this task, we found that the magnitude of baseline LC activity following the rule change was prominently correlated with the degree of task switching. Specifically, higher baseline activity upon the rule shift was associated with faster behavioral switching (more flexible), whereas lower baseline activity upon the rule shift was associated with slower switching (less flexible). These findings are further strengthened by perturbation experiments where optogenetic enhancement of baseline activity improved task performance and accelerated task switching.

Prestimulus baseline LC activity (commonly referred to as tonic activity in the literature) exhibited a significant increase during fast switching, in line with similar magnitude (<1 spike/s) of firing rate changes associated with behavioral states or rule shifts in prior work (e.g., Aston-Jones and Bloom, 1981; Aston-Jones et al., 1997; Usher et al., 1999; Xiang et al., 2019). Given the ~1 spike/s baseline firing rate in our study (Figure 2G) and the monotonic relationship between LC spiking and the release of noradrenaline in terminal fields (Berridge and Abercrombie, 1999), a ~50% increase of spiking activity from hundreds of neurons is likely to exert a significant downstream effect. Importantly, we uncovered that such activity exhibited a graded, negative relationship with the degree of behavioral switching. We also noted that LC neurons transiently responded to the auditory tone and whisker stimulation (commonly referred to as phasic activity), and found relatively weak relationships between such responses and task switching (Figure S5).

Generally speaking, faster switching to the new rule is in line with the concept of enhanced exploratory behavior or disengagement from the current task (Aston-Jones and Cohen, 2005; Kane et al., 2017; Koralek and Costa, 2021). However, enhanced exploration/task disengagement is not necessarily equivalent to being able to switch to and follow a new rule. Specifically, our perturbation data support recent work in the head-fixed setting, showing that activating the LC facilitated auditory reversal learning (Glennon et al., 2019; Martins and Froemke, 2015). A major distinction in our study is that the current task is essentially a continuous reversal task, and prior to LC stimulation mice had been trained to adapt to multiple reversal stages (blocks) within single sessions, similar to the task structure of a recent work (Chevée et al., 2021). This task design allows us to assess the relationship between LC activity and rapid, “real-time” behavioral switching within individual sessions. The association between baseline LC activity and flexible task switching was transient (~20 trials, equivalent to 2–3 minutes; Figure 2F; also see Aston-Jones et al., 1997). Second, LC optical stimulation was delivered in a subset of trials (a total of ~20–30 trials per block; STAR Methods) and the behavioral improvement was present from the first stimulation session (day 1; Figure 3C). As a result, long-term plasticity mechanisms, such as structural synaptic changes, are unlikely to underlie such rapid associations between LC activity and behavioral switching. Nevertheless, it is worth noting that in a recent study where LC stimulation was paired with the target tone in a relatively long-term fashion, rats were found to better suppress their responses to non-target tones (Glennon et al., 2019), consistent with an increase of correct rejection rate in our findings. Together, these studies suggest that LC activity facilitates behavioral flexibility across different timescales, likely through different mechanisms.

How does LC activity drive behavioral flexibility? This remains a major challenge in the field. Ample prior research has shown that noradrenergic (NA) signaling from the LC modulates neuronal responses to sensory stimuli in various sensory-related brain structures (Berridge and Waterhouse, 2003; McBurney-Lin et al., 2019; Waterhouse and Navarra, 2019). Thus, the transient increase of LC activity following the rule change may modulate neuronal responses to the new Go and/or NoGo stimulus (Devilbiss and Waterhouse, 2004; Devilbiss et al., 2006; Martins and Froemke, 2015; Rodenkirch et al., 2019) to better separate signal and noise representations. The fact that LC stimulation only affected behavioral responses to the NoGo stimulus (correct rejection) is consistent with the learning

progression of the mice, which appeared to be associated with an increase of correct rejection rate, rather than hit rate (Figure 1D). Such behavioral effects suggest more specific mechanisms that may attenuate the encoding or propagation of the NoGo stimulus, such as LC modulation of the sensorimotor cortices on the NoGo side (e.g., Aruljothi et al., 2020; Zareian et al., 2021). Another possibility is that LC-NA signaling facilitates the reshaping of tactile stimulus representation to more effectively influence behavior (Ruff and Cohen, 2016, 2019). On the other hand, decades of work has established the importance of the prefrontal cortex (PFC) in behavioral flexibility (Le Merre et al., 2021; Miller and Cohen, 2001; Uddin, 2021), and LC-NA signaling heavily influences PFC functions and behavior (Arnsten and Li, 2004; Arnsten et al., 2012; Bari et al., 2020; Cope et al., 2019; Ramos and Arnsten, 2007; Tervo et al., 2014). Transient changes in LC activity may dynamically modulate synaptic efficacy and recurrent activity in the PFC to affect top-down regulation of the propagation of sensorimotor signals (Arnsten et al., 2012; Zagha, 2020) and to facilitate reorienting behavior (Sara and Bouret, 2012). Future experiments with simultaneous recordings from LC-NA and sensorimotor/executive areas will elucidate how LC-NA activity modulates bottom-up processing and top-down commands to influence behavioral flexibility.

Limitations of the study

We developed a relatively simple rule-shift task to probe LC's function in head-fixed mice. Nevertheless, this task appears to be more demanding and challenging for the mice to learn compared with tactile detection tasks without a rule switch (e.g., Aruljothi et al., 2020; Yang et al., 2016), as mice can typically perform the latter at >70% within 2 weeks of training. Our task design follows a history of using deterministic behavioral paradigms to assess flexible/adaptive decision making, such as the Wisconsin Card Sorting Task, the Intra-Extra Dimensional Set Shift Task, the Attentional Set-Shifting Task, and more recent head-fixed paradigms in mice (Banerjee et al., 2020; Berg, 1948; Birrell and Brown, 2000; Reinert et al., 2021; Roberts et al., 1988; Spellman et al., 2021). However, our task does not involve a probabilistic component and thus are not sensitive to tease apart specific processes such as surprise versus change (cf. Dayan and Yu, 2006; Yu and Dayan, 2005).

We optogenetically activated LC neurons at a higher frequency than the measured firing rate during behavior. As described earlier, this is meant to drive LC to safely surpass the "noisy" range of baseline activity, as well as to compensate the limiting factor that optical stimulation only activates a subset of neurons. However, future experiments are needed to test whether graded LC activation and inhibition can induce graded behavioral effects.

STAR★METHODS

RESOURCE AVAILABILITY

Lead contact—Further information and requests for resources and reagents should be directed to and will be fulfilled by the lead contact, Hongdian Yang (hongdian@ucr.edu).

Materials availability—This study did not generate new unique reagents.

Data and code availability

- All data reported in this paper will be shared by the lead contact upon request.
- All original code has been deposited at Zenodo and is publicly available as of the date of publication. DOIs are listed in the key resources table.
- Any additional information required to reanalyze the data reported in this paper is available from the lead contact upon request.

EXPERIMENTAL MODEL AND SUBJECT DETAILS

Mice—All procedures were performed in accordance with protocols approved by UC Riverside Animal Care and Use Committee (AUP 20190031). Mice were DBH-Cre (B6.FVB(Cg)-Tg(Dbh-cre) KH212Gsat/Mmucd, 036778-UCD, MMRRC); Ai32 (RCL-ChR2(H134R)/EYFP, 024109, JAX), singly housed in a vivarium with a reversed light-dark cycle (9a-9p). A total of 18 male and female mice were included (8 male, 10 female).

METHOD DETAILS

Surgery—Mice of 8–12 weeks old were implanted with titanium headposts, leaving a window open above the left cerebellum for subsequent tetrode implants. Custom tetrode microdrives were made with eight tetrode wires surrounding an optic fiber (0.39 NA, 200 um core) to make extracellular recordings from opto-tagged LC neurons (Cohen et al., 2012; Yang et al., 2016, 2021). Each tetrode comprised four nichrome wires (100–300 kW). The microdrive was implanted targeting the left LC. A ~1 mm diameter craniotomy was made (centered at 5.2 mm caudal and 0.85 mm lateral relative to bregma) for implanting the tetrodes to a depth of 2.7 mm relative to the brain surface. The microdrive was advanced in steps of ~100 μm each day until reaching LC. Mice were then allowed to recover for at least 72 h before water restriction and behavior training.

Behavioral training—Mice were water restricted to 1mL/day for at least seven days prior to behavioral training. Behavioral tasks were controlled via a custom-based Arduino hardware and software and acquired in WaveSurfer (https://www.janelia.org/open-science/wavesurfer), and one behavioral session was performed per day. Mice were first trained to a modified version of the Go/NoGo single-whisker detection task (Yang et al., 2016; McBurney-Lin et al., 2020). In brief, mice reported the presence of a brief deflection (0.2-s, 25-Hz sinusoidal) to either the right or the left C2 whisker by licking a water port during a 1-s response window. On Go trials, stimulation of the right or the left whisker was delivered in alternating blocks (e.g., first 100 trials, stimuli were presented to the right whisker, following 100 trials to the left whisker, etc.). On NoGo trials, no whisker stimulation was delivered, and mice were trained to withhold licking. Mice usually achieved >75% overall performance within 7 days. Mice were then introduced to the second stage of training, in which an identical whisker deflection was presented on NoGo trials on the contralateral side to the Go stimulus (e.g., left stimulus: Go; right stimulus: NoGo). Similar to the first stage of training, the stimuli were presented in block structures, with the Go stimulus alternating from left to right whiskers. Early during this stage of training, a single rule switch was implemented, and each block consisted of 200 trials. The first block rule was randomly assigned as either left Go/right NoGo or right Go/left NoGo. As the mouse became more

proficient in switching, the blocks were shortened progressively and additional 1–2 rule changes added. Therefore, as mice learned the task, more rule changes were introduced into single sessions. The mice in this study could execute between one and three rule changes in a session.

The beginning of each block consisted of a 'cueing window', which was a period of 5–10 consecutive Go trials where whisker stimulation was paired with water delivery, designed to facilitate adaptation to the new rule. A 0.1-s auditory cue (8 kHz, ~80 dB SPL) signaled the start of each trial, followed by a 1.5-s delay before whisker stimulation. If mice licked in this delay window, the trial was aborted and the next trial began after a 5–10 s timeout. Ambient white noise (cut off at 40 kHz, ~80 dB SPL) was played continuously to mask any potential cues that can be associated with the task. Go and NoGo trials represented 90% of all trials. Catch trials represented the remaining 10%, in which no whisker stimulation was presented, and mice were trained to withhold licking. On Go trials, the Go stimulus for the current block was delivered, and mice were expected to report its presence by licking the water port within a 1-s window immediately following stimulus cessation. Correct responses to Go stimulus presentation were qualified as 'hit' trials and rewarded with a water drop (~5uL). Withholding licking to Go stimulus were qualified as 'miss' trials. Withholding licking to NoGo stimulus and on catch trials were unrewarded and qualified as 'correct rejection'. Licking to NoGo stimulus and on catch trials were qualified as 'false alarm' and punished with a 5-s timeout. If the mouse licked again within the timeout period but at least 1-s after the initial response, there was a subsequent 5-s punishment, with up to three consecutive timeouts allowed per trial. To further assist mice to suppress licking to the NoGo stimulus, a NoGo trial was designed to follow a 'false alarm' trial (Aruljothi et al., 2020), and up to 4 consecutive NoGo trials were allowed to occur. As a result, behavioral sessions typically consisted of more NoGo trials than Go trials (~55% vs. 45%).

Electrophysiology—Once mice reached the performance threshold (65%, block 2), the microdrive was advanced at regular intervals (75 um/day) towards LC. Thirty-four single-unit recording sessions (cluster quality measure Lratio: 0.01 ± 0.005; firing rate: 2.44 ± 0.30 spikes/s; percent ISI <10 ms: 1.21% ± 0.42%) from six mice performing the rule-shift task were extracted using MClust (Redish, 2014), along with synchronous recording of the left pupil. In each session a single unit was recorded, and we did not distinguish whether the same unit or different units were recorded across multiple sessions from the same mouse. We used long pulses (0.3-s) for tagging as recent work showed that a subset of LC neurons cannot be excited by short pulses (Hickey et al., 2014; Li et al., 2016). Units in majority of the recording sessions had short latency to optogenetic stimulation (6.0 (4.4, 9.6) ms, median (IQR)). A small fraction of recordings had response latency longer than 10 ms (21%, 7 out of 34), consistent with previous reports (Hickey et al., 2014; Li et al., 2016). However, main results in Figure 2 regarding the relationship between LC activity and flexible task switching are robust when the 7 long latency recordings are excluded from analysis (for example, statistics in Figure 2I would become: correlation coefficient = −0.39, p = 0.01).

Optogenetic stimulation and pupil tracking—Optogenetic perturbation experiments were acquired from seven mice (4 test, 3 control) that had been trained for >4 weeks on

the rule-shift task with switch performance consistently below the 65% threshold. Prior to optogenetic experiments, placement of the optic fiber was assessed by pupil responses to optical stimulation (10-ms pulses, 10 Hz, 10 mW). Optogenetic stimulation was delivered using a 450 nm blue diode laser (UltraLasers, MDL-III-450–200mW) and controlled by WaveSurfer. The mating between sleeve and ferrule was covered with polymer clay to prevent light leakage. Stimulation of LC neurons was delivered on Go trials during a 0.5-s window prior to whisker stimulation onset. Video of the left pupil was acquired at 20 Hz using a Basler acA1300–200um camera and Pylon software. Pupil diameter was measured offline using DeepLabCut (Mathis et al., 2018). Electrophysiology recording, pupil tracking, and optogenetic stimulation were synchronized via a common TTL pulse train.

Immunohistochemistry—At the conclusion of all experiments, electrolytic lesions were made and brains perfused with PBS, followed by 4% PFA. The brains were post-fixed in 4% PFA overnight, then cut into 100 um coronal sections and stained for Tyrosine Hydroxylase (TH, Thermo-fisher OPA1–04050 and A-11012) and EGFP (Thermo-fisher A-11039).

QUANTIFICATION AND STATISTICAL ANALYSIS

Data were reported as mean ± SEM unless otherwise noted. We did not use statistical methods to predetermine sample sizes. Sample sizes were similar to those reported in the field. We assigned mice to experimental groups arbitrarily, without randomization or blinding. Unless otherwise noted, statistical tests were two-tailed Wilcoxon signed-rank (paired) or rank-sum (unpaired) when sample sizes were >7. When sample sizes were ≤7, statistical tests were two-tailed paired or unpaired t test, respectively.

Data analysis - behavior—Switch performance (fraction correct) was quantified in blocks other than the first block (block 1) in a session. To compute the behavioral switch point in a block, task performance was first quantified using a 50-trial moving window. Behavioral switch point was defined as the beginning of the moving window within which the average task performance surpassed 85% threshold. Importantly, behavioral switch point of 1 trial meant that task performance surpassed the threshold within the first 50-trial window, and it did not necessarily mean that the mouse already switched to the new rule on trial 1. If this criterion was never met, i.e., task performance in the 50-trial moving window never reached 85% threshold within the block, switch point was set as the total number of trials in that block. For Figure 1D, switch performance was quantified in block 2 as early training sessions only had 2 blocks. For Figures 1F–1H, 84 blocks from 59 sessions of 11 mice were included.

Data analysis - electrophysiology—For Figure 2, baseline LC activity was quantified in a 1-s window prior to whisker stimulation onset. 20 trials before the rule change (i.e., last 20 trials in the previous block) were considered as the Before period, and 20 trials after the rule change were considered as the After period. For Figure 2E, the average firing rate in the Before and After periods was smoothed using a 150-ms window. Figure 2F quantified the 10-trial averaged baseline firing rate for ±50 trials from the rule change. The change (Δ) in baseline firing rate was calculated as baseline LC activity in the Before period subtracted from the After period (After - Before). 14 blocks from 7 sessions of 3 mice were included

in Figures 2G and 2H, 1 fast block and 1 slow block pair per session. Contributions from individual mice were 2 sessions, 1 session, and 4 sessions. Making the number of sessions from the most contributed mouse more comparable to others (i.e., reducing from 4 sessions to 2 sessions) did not affect the results in Figures 2G and 2H (For example, statistics in Figure 2H would become: $p = 0.012$). For Figures 2I and 2J, 49 blocks from 34 sessions of 6 mice were presented, a subset of the sessions in Figures 1F–1H. Contributions from individual mice were 7 sessions, 6 session, 14 sessions, 1 session, 3 sessions and 3 sessions. Making the number of sessions from the most contributed mouse more comparable to others did not affect the results in Figures 2I and 2J. Specifically, we systematically subsampled the sessions from the first 3 mice by randomly drawing 7 sessions (out of 14, thus contributions from each mouse become 7, 6, 7, 1, 3, 3), or randomly drawing 6 sessions (out of 7 and 14, thus contributions from each mouse become 6, 6, 6, 1, 3, 3), or randomly drawing 5 sessions (out of 7, 6, and 14, thus contributions from each mouse become 5, 5, 5, 1, 3, 3) from each mouse to make their contributions more similar to the other 3 mice. In each condition, we randomly draw from the sessions of each mouse 10 times and report the correlation coefficient and p value. 7 sessions: c.c. = -0.41 ± 0.005, $p = 0.013 \pm 0.002$; 6 sessions: c.c. = -0.40 ± 0.006, $p = 0.023 \pm 0.003$; 5 sessions: c.c. = -0.40 ± 0.010, $p = 0.034 \pm 0.005$. Similarly, when in each iteration we randomly draw 4, 5, or 6 sessions from each of the first 3 mice, c.c. = -0.39 ± 0.008, $p = 0.036 \pm 0.005$.

Data analysis - optogenetic stimulation—In Figure 3, optogenetic stimulation began at the beginning of each block and ended 50 trials after the cueing trials. Stimulation (10-ms pulse train at 10 Hz and 10 mW) was delivered on Go trials only, starting at 0.5 s before whisker stimulation onset and ending at the onset. Switch performance and switch point were quantified in block 2 as majority of the sessions had 2 blocks. 5 consecutive baseline sessions (no stimulation) and 5 consecutive stimulation sessions from each mouse were included for analysis (1 session per day). For Figures 3D and 3E, analyses were performed within individual mice separately. For Figures 3F–3I, sessions were pooled from all mice in each condition (i.e., 20 sessions from the test group (5 consecutive sessions per mouse, 4 mice) and 15 sessions from the control group (5 consecutive sessions per mouse, 3 mice) in each condition).

Supplementary Material

Refer to Web version on PubMed Central for supplementary material.

ACKNOWLEDGEMENTS

We thank Martin Riccomagno, Sachiko Haga-Yamanaka, and the anonymous reviewers for commenting on the manuscript. E.Z. was supported by National Institutes of Health (NIH) grant R01NS107599. H.Y. was supported by University of California, Riverside (UCR) startup, Klingenstein-Simons Fellowship Awards in Neuroscience, and NIH grants R01NS107355 and R01NS112200.

REFERENCES

Allen WE, Chen MZ, Pichamoorthy N, Tien RH, Pachitariu M, Luo L, and Deisseroth K (2019). Thirst regulates motivated behavior through modulation of brainwide neural population dynamics. Science 364, 253. 10.1126/science.aav3932. [PubMed: 30948440]

Arnsten A, and Li B (2004). Neurobiology of executive functions: catecholamine influences on prefrontal cortical functions. Biol. Psychiatry 57, 1377–1384. 10.1016/j.bps.2004.08.019.

Arnsten AFTT, Wang MJ, and Paspalas CD (2012). Neuromodulation of thought: flexibilities and vulnerabilities in prefrontal cortical network synapses. Neuron 76, 223–239. 10.1016/j.neuron.2012.08.038. [PubMed: 23040817]

Aruljothi K, Marrero K, Zhang Z, Zareian B, and Zagha E (2020). Functional localization of an attenuating filter within cortex for a selective detection task in mice. J. Neurosci. 40. 10.1523/jneurosci.2993-19.2020.

Aston-Jones G, and Bloom FE (1981). Activity of norepinephrine-containing locus coeruleus neurons in behaving rats anticipates fluctuations in the sleep-waking cycle. J. Neurosci. 1, 876–886. 10.1523/jneurosci.01-08-00876.1981. [PubMed: 7346592]

Aston-Jones G, and Cohen JD (2005). An integrative theory of locus coeruleus-norepinephrine function: adaptive gain and optimal performance. Annu. Rev. Neurosci. 28, 403–450. 10.1146/annurev.neuro.28.061604.135709. [PubMed: 16022602]

Aston-Jones G, Rajkowski J, Kubiak P, and Alexinsky T (1994). Locus coeruleus neurons in monkey are selectively activated by attended cues in a vigilance task. J. Neurosci. 14, 4467–4480. 10.1523/jneurosci.14-07-04467.1994. [PubMed: 8027789]

Aston-Jones G, Rajkowski J, and Kubiak P (1997). Conditioned responses of monkey locus coeruleus neurons anticipate acquisition of discriminative behavior in a vigilance task. Neuroscience 80, 697–715. 10.1016/S0306-4522(97)00060-2. [PubMed: 9276487]

Aston-Jones G, Rajkowski J, and Cohen J (1999). Role of locus coeruleus in attention and behavioral flexibility. Biol. Psychiatry 46, 1309–1320. 10.1016/S0006-3223(99)00140-7. [PubMed: 10560036]

Banerjee A, Parente G, Teutsch J, Lewis C, Voigt FF, and Helmchen F (2020). Value-guided remapping of sensory cortex by lateral orbitofrontal cortex. Nature 585, 245–250. 10.1038/s41586-020-2704-z. [PubMed: 32884146]

Bari A, Xu S, Pignatelli M, Takeuchi D, Feng J, Li Y, and Tonegawa S (2020). Differential attentional control mechanisms by two distinct noradrenergic coeruleo-frontal cortical pathways. Proc. Natl. Acad. Sci. USA 117, 29080–29089. 10.1073/pnas.2015635117. [PubMed: 33139568]

Bartolo R, and Averbeck BB (2020). Prefrontal cortex predicts state switches during reversal learning. Neuron 106, 1044–1054.e4. 10.1016/j.neuron.2020.03.024. [PubMed: 32315603]

Berditchevskaia A, Cazé RD, and Schultz SR (2016). Performance in a GO/NOGO perceptual task reflects a balance between impulsive and instrumental components of behaviour. Sci. Rep. 6, 1–15. 10.1038/srep27389. [PubMed: 28442746]

Berg EA (1948). A simple objective technique for measuring flexibility in thinking. J. Gen. Psychol. 39, 15–22. 10.1080/00221309.1948.9918159. [PubMed: 18889466]

Berridge CW, and Abercrombie ED (1999). Relationship between locus coeruleus discharge rates and rates of norepinephrine release within neocortex as assessed by in vivo microdialysis. Neuroscience 93, 1263–1270. 10.1016/S0306-4522(99)00276-6. [PubMed: 10501450]

Berridge CW, and Waterhouse BD (2003). The locus coeruleus-noradreneergic system: modulation of behavioral state and state-dependent cognitive processes. Brain Res. Rev. 42, 33–84. 10.1016/S0165-0173(03)00143-7. [PubMed: 12668290]

Birrell JM, and Brown VJ (2000). Medial frontal cortex mediates perceptual attentional set shifting in the rat. J. Neurosci. 20, 4320–4324. 10.1523/JNEUROSCI.20-11-04320.2000. [PubMed: 10818167]

Bouret S, and Sara SJ (2004). Reward expectation, orientation of attention and locus coeruleus-medial frontal cortex interplay during learning. Eur. J. Neurosci. 20, 791–802. 10.1111/j.1460-9568.2004.03526.x. [PubMed: 15255989]

Chevée M, Finkel EA, Kim S-J, O'Connor DH, and Brown SP (2021). Neural activity in the mouse claustrum in a cross-modal sensory selection task. Neuron, 1–16. 10.1016/j.neuron.2021.11.013. [PubMed: 33412092]

Clayton EC, Rajkowski J, Cohen JD, and Aston-Jones G (2004). Phasic activation of monkey locus ceruleus neurons by simple decisions in a forcedchoice task. J. Neurosci. 24, 9914–9920. 10.1523/JNEUROSCI.2446-04.2004. [PubMed: 15525776]

Cohen JY, Haesler S, Vong L, Lowell BB, and Uchida N (2012). Neuron-type-specific signals for reward and punishment in the ventral tegmental area. Nature 482, 85–88. 10.1038/nature10754. [PubMed: 22258508]

Cope ZA, Vazey EM, Floresco SB, and Aston Jones GS (2019). DREADD-mediated modulation of locus coeruleus inputs to mPFC improves strategy set-shifting. Neurobiol. Learn. Mem. 161, 1–11. 10.1016/j.nlm.2019.02.009. [PubMed: 30802603]

Dayan P, and Yu AJ (2006). Phasic norepinephrine: a neural interrupt signal for unexpected events. Netw. Comput. Neural Syst. 17, 335–350. 10.1080/09548980601004024.

Devauges V, and Sara SJ (1990). Activation of the noradrenergic system facilitates an attentional shift in the rat. Behav. Brain Res. 39, 19–28. 10.1016/0166-4328(90)90118-X. [PubMed: 2167690]

Devilbiss DM, and Waterhouse BD (2004). The effects of tonic locus ceruleus output on sensory-evoked responses of ventral posterior medial thalamic and barrel field cortical neurons in the awake rat. J. Neurosci. 24, 10773–10785. 10.1523/JNEUROSCI.1573-04.2004. [PubMed: 15574728]

Devilbiss DM, Page ME, and Waterhouse BD (2006). Locus ceruleus regulates sensory encoding by neurons and networks in waking animals. J. Neurosci. 26, 9860–9872. 10.1523/JNEUROSCI.1776-06.2006. [PubMed: 17005850]

Durstewitz D, Vittoz NM, Floresco SB, and Seamans JK (2010). Abrupt transitions between prefrontal neural ensemble states accompany behavioral transitions during rule learning. Neuron 66, 438–448. 10.1016/j.neuron.2010.03.029. [PubMed: 20471356]

Glennon E, Carcea I, Martins ARO, Multani J, Shehu I, Svirsky MA, and Froemke RC (2019). Locus coeruleus activation accelerates perceptual learning. Brain Res. 1709, 39–49. 10.1016/j.brainres.2018.05.048. [PubMed: 29859972]

Hickey L, Li Y, Fyson SJ, Watson TC, Perrins R, Hewinson J, Teschemacher AG, Furue H, Lumb BM, and Pickering AE (2014). Optoactivation of locus ceruleus neurons evokes bidirectional changes in thermal nociception in rats. J. Neurosci. 34, 4148–4160. 10.1523/JNEUROSCI.4835-13.2014. [PubMed: 24647936]

Janitzky K, Lippert MT, Engelhorn A, Tegtmeier J, Goldschmidt J, Heinze H-J, and Ohl FW (2015). Optogenetic silencing of locus coeruleus activity in mice impairs cognitive flexibility in an attentional set-shifting task. Front. Behav. Neurosci. 9, 1–8. 10.3389/fnbeh.2015.00286. [PubMed: 25653603]

Kane GA, Vazey EM, Wilson RC, Shenhav A, Daw ND, Aston-Jones G, and Cohen JD (2017). Increased locus coeruleus tonic activity causes disengagement from a patch-foraging task. Cogn. Affect. Behav. Neurosci. 17, 1073–1083. 10.3758/s13415-017-0531-y. [PubMed: 28900892]

Koralek AC, and Costa RM (2021). Dichotomous dopaminergic and noradrenergic neural states mediate distinct aspects of exploitative behavioral states. Sci. Adv. 7, 1–13. 10.1126/sciadv.abh2059.

Lapiz MDS, and Morilak DA (2006). Noradrenergic modulation of cognitive function in rat medial prefrontal cortex as measured by attentional set shifting capability. Neuroscience 137, 1039–1049. 10.1016/j.neuroscience.2005.09.031. [PubMed: 16298081]

Li Y, Hickey L, Perrins R, Werlen E, Patel AA, Hirschberg S, Jones MW, Salinas S, Kremer EJ, and Pickering AE (2016). Retrograde optogenetic characterization of the pontospinal module of the locus coeruleus with a canine adenoviral vector. Brain Res. 1641, 274–290. 10.1016/j.brainres.2016.02.023. [PubMed: 26903420]

Martins ARO, and Froemke RC (2015). Coordinated forms of noradrenergic plasticity in the locus coeruleus and primary auditory cortex. Nat. Neurosci. 18, 1483–1492. 10.1038/nn.4090. [PubMed: 26301326]

Mathis A, Mamidanna P, Cury KM, Abe T, Murthy VN, Mathis MW, and Bethge M (2018). DeepLabCut: markerless pose estimation of user-defined body parts with deep learning. Nat. Neurosci. 21, 1281–1289. 10.1038/s41593-018-0209-y. [PubMed: 30127430]

McBurney-Lin J, Lu JJ, Zuo YY, and Yang H (2019). Locus coeruleus-norepinephrine modulation of sensory processing and perception: a focused review. Neurosci. Biobehav. Rev. 105, 190–199. 10.1016/j.neubiorev.2019.06.009. [PubMed: 31260703]

McBurney-Lin J, Sun Y, Tortorelli LS, Nguyen QAT, Haga-Yamanaka S, and Yang H (2020). Bidirectional pharmacological perturbations of the noradrenergic system differentially affect tactile detection. Neuropharmacology 174, 108151. 10.1016/j.neuropharm.2020.108151. [PubMed: 32445638]

Megemont M, McBurney-Lin J, and Yang H (2022). Pupil diameter is not an accurate real-time readout of locus coeruleus activity. Elife 11, 1–17. 10.7554/eLife.70510.

Le Merre P, Ährlund-Richter S, and Carlén M (2021). The mouse prefrontal cortex: unity in diversity. Neuron, 1–20. 10.1016/j.neuron.2021.03.035. [PubMed: 33412092]

Miller EK, and Cohen JD (2001). An integrative theory of prefrontal cortex function. Annu. Rev. Neurosci. 24, 167–202. 10.1146/annurev.neuro.24.1.167. [PubMed: 11283309]

Privitera M, Ferrari KD, von Ziegler LM, Sturman O, Duss SN, Floriou-Servou A, Germain P, Vermeiren Y, Wyss MT, De Deyn PP, et al. (2020). A complete pupillometry toolbox for real-time monitoring of locus coeruleus activity in rodents. Nat. Protoc. 10.1038/s41596-020-0324-6.

Rajkowski J, Kubiak P, and Aston-Jones G (1994). Locus coeruleus activity in monkey: phasic and tonic changes are associated with altered vigilance. Brain Res. Bull. 35, 607–616. 10.1016/0361-9230(94)90175-9. [PubMed: 7859118]

Rajkowski J, Majczynski H, Clayton E, and Aston-Jones G (2004). Activation of monkey locus coeruleus neurons varies with difficulty and performance in a target detection task. J. Neurophysiol. 92, 361–371. 10.1152/jn.00673.2003. [PubMed: 15028743]

Ramos BP, and Arnsten AFTT (2007). Adrenergic pharmacology and cognition: focus on the prefrontal cortex. Pharmacol. Ther. 113, 523–536. 10.1016/j.pharmthera.2006.11.006. [PubMed: 17303246]

Redish AD (2014). MClust Spike Sorting Toolbox Documentation for Version 4.4.

Reinert S, Hübener M, Bonhoeffer T, and Goltstein PM (2021). Mouse prefrontal cortex represents learned rules for categorization. Nature 593, 411–417. 10.1038/s41586-021-03452-z. [PubMed: 33883745]

Rich EL, and Shapiro M (2009). Rat prefrontal cortical neurons selectively code strategy switches. J. Neurosci. 29, 7208–7219. 10.1523/JNEUROSCI.6068-08.2009. [PubMed: 19494143]

Roberts AC, Robbins TW, and Everitt BJ (1988). The effects of intradimensional and extradimensional shifts on visual discrimination learning in humans and non-human primates. Q. J. Exp. Psychol. B 40, 321–341. 10.1080/14640748808402328. [PubMed: 3145534]

Rodenkirch C, Liu Y, Schriver BJ, and Wang Q (2019). Locus coeruleus activation enhances thalamic feature selectivity via norepinephrine regulation of intrathalamic circuit dynamics. Nat. Neurosci. 22, 120–133. 10.1038/s41593-018-0283-1. [PubMed: 30559472]

Ruff DA, and Cohen MR (2016). Attention increases spike count correlations between visual cortical areas. J. Neurosci. 36, 7523–7534. 10.1523/JNEUROSCI.0610-16.2016. [PubMed: 27413161]

Ruff DA, and Cohen MR (2019). Simultaneous multi-area recordings suggest that attention improves performance by reshaping stimulus representations. Nat. Neurosci. 22, 1669–1676. 10.1038/s41593-019-0477-1. [PubMed: 31477898]

Sara SJ, and Bouret S (2012). Orienting and reorienting: the locus coeruleus mediates cognition through arousal. Neuron 76, 130–141. 10.1016/j.neuron.2012.09.011. [PubMed: 23040811]

Spellman T, Svei M, Kaminsky J, Manzano-Nieves G, and Liston C (2021). Prefrontal deep projection neurons enable cognitive flexibility via persistent feedback monitoring. Cell 184, 2750–2766.e17. 10.1016/j.cell.2021.03.047. [PubMed: 33861951]

Tervo DGR, Proskurin M, Manakov M, Kabra M, Vollmer A, Branson K, and Karpova AY (2014). Behavioral variability through stochastic choice and its gating by anterior cingulate cortex. Cell 159, 21–32. 10.1016/j.cell.2014.08.037. [PubMed: 25259917]

Uddin LQ (2021). Cognitive and behavioural flexibility: neural mechanisms and clinical considerations. Nat. Rev. Neurosci. 10.1038/s41583-021-00428-w.

Usher M, Cohen JD, Servan-Schreiber D, Rajkowski J, and Aston-Jones G (1999). The role of locus coeruleus in the regulation of cognitive performance. Science 283, 549–554. 10.1126/science.283.5401.549. [PubMed: 9915705]

Waterhouse BD, and Navarra RL (2019). The locus coeruleus-norepinephrine system and sensory signal processing: a historical review and current perspectives. Brain Res. 1709, 1–15. 10.1016/j.brainres.2018.08.032. [PubMed: 30179606]

Xiang L, Harel A, Gao HY, Pickering AE, Sara SJ, and Wiener SI (2019). Behavioral correlates of activity of optogenetically identified locus coeruleus noradrenergic neurons in rats performing T-maze tasks. Sci. Rep. 9, 1–13. 10.1038/s41598-018-37227-w. [PubMed: 30626917]

Yang H, Kwon SE, Severson KS, and O'Connor DH (2016). Origins of choice-related activity in mouse somatosensory cortex. Nat. Neurosci. 19, 127–134. 10.1038/nn.4183. [PubMed: 26642088]

Yang H, Bari BA, Cohen JY, and O'Connor DH (2021). Locus coeruleus spiking differently correlates with S1 cortex activity and pupil diameter in a tactile detection task. Elife 10, 1–14. 10.7554/eLife.64327.

Yu AJ, and Dayan P (2005). Uncertainty, neuromodulation, and attention. Neuron 46, 681–692. 10.1016/j.neuron.2005.04.026. [PubMed: 15944135]

Zagha E (2020). Shaping the cortical landscape: functions and mechanisms of top-down cortical feedback pathways. Front. Syst. Neurosci. 14, 1–17. 10.3389/fnsys.2020.00033. [PubMed: 32116576]

Zagha E, Erlich JC, Lee S, Lur G, O'Connor DH, Steinmetz NA, Stringer C, Yang H, O'Connor DH, Steinmetz NA, et al. (2022). The importance of accounting for movement when relating neuronal activity to sensory and cognitive processes. J. Neurosci. 42, 1375–1382. 10.1523/JNEUROSCI.1919-21.2021. [PubMed: 35027407]

Zareian B, Zhang Z, and Zagha E (2021). Cortical localization of the sensory-motor transformation in a whisker detection task in mice. eNeuro 8, 1–14. 10.1523/ENEURO.0004-21.2021.

Highlights

- A tactile-based rule-shift detection task tests flexible behavioral switching
- Trained mice exhibit different degrees of switching behavior
- LC baseline activity prominently correlates with the degree of behavioral switching
- Enhancing LC baseline activity facilitates rule switching

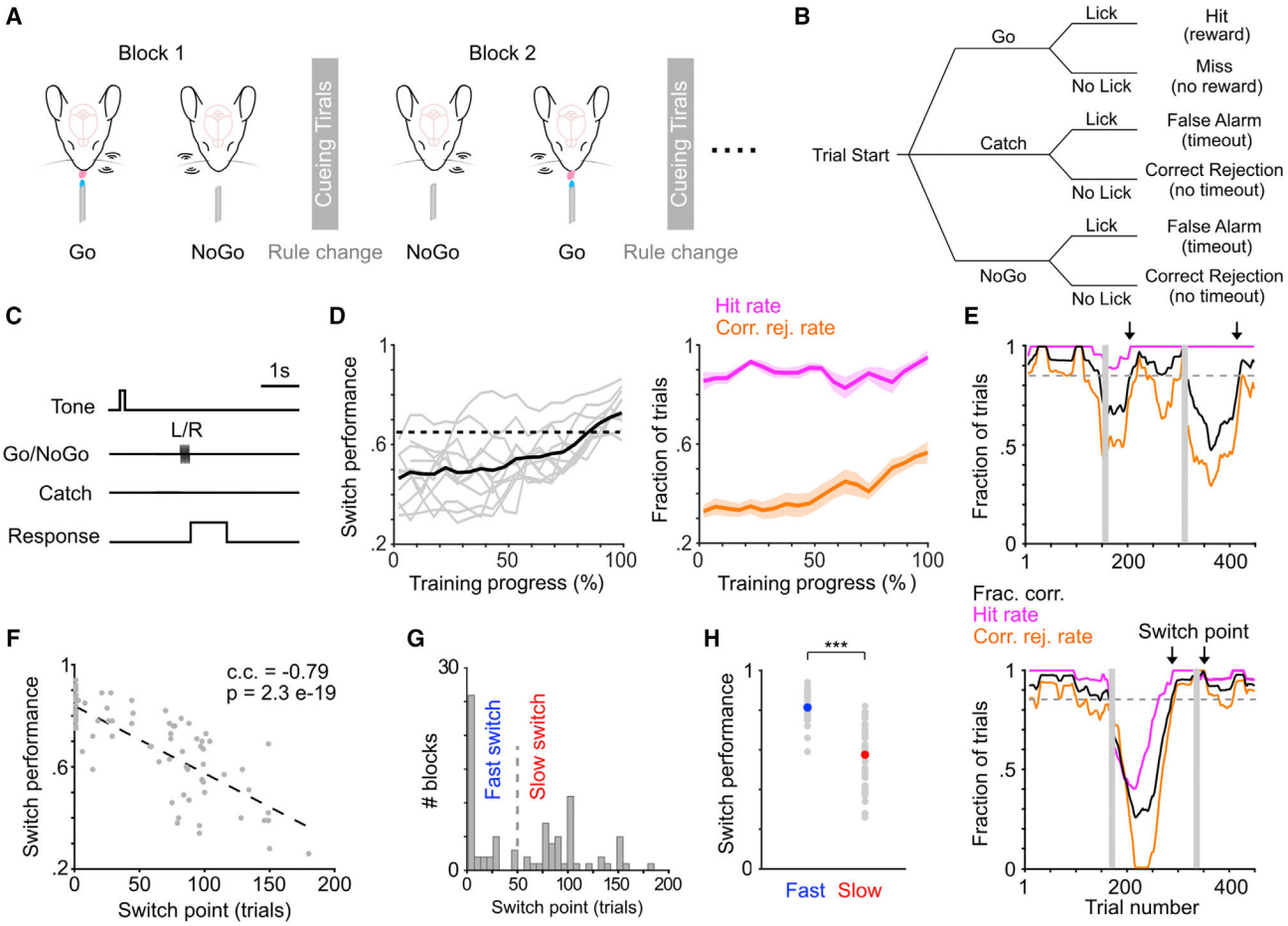

Figure 1. A novel tactile-based rule-shift detection task to probe flexible task switching

(A–C) Schematic of the task paradigm in head-fixed mice (A), with illustrations of trial types (B) and trial structure (C).

(D) Left: switch performance (fraction correct in block 2) during training (n = 11 mice, gray curves). Training progressions (days) across mice are normalized. Unnormalized data shown in Figure S1A. Solid black curve represents group mean. Dotted horizontal line indicates 65% threshold. Right: hit rate and correct rejection rate during training (mean ± SEM).

(E) Two example behavioral sessions to illustrate different degrees of behavioral switching. Top: early/fast switch in block 2 and late/slow switch in block 3. Bottom: late switch in block 2 and early switch in block 3. Arrows indicate when moving averaged switch performance (black curve) exceeds 85% (dashed line). Vertical gray bars indicate cueing trials.

(F) The relationship between behavioral switch point and switch performance. c.c., Pearson correlation coefficient. Eighty-four blocks from 59 sessions of 11 mice, same data used in (G) and (H).

(G) Histogram of behavioral switch point. We used 50 trials (dashed line) to separate fast and slow switch blocks.

(H) Switch performance for fast and slow switch blocks shown in (G). Fast (40 blocks) versus slow (44 blocks): 0.81 ± 0.011 versus 0.58 ± 0.022, p = 2.9e-12, rank sum = 2,480,

two-tailed Wilcoxon rank-sum test. Gray dots represent individual blocks, blue and red dots represent mean.

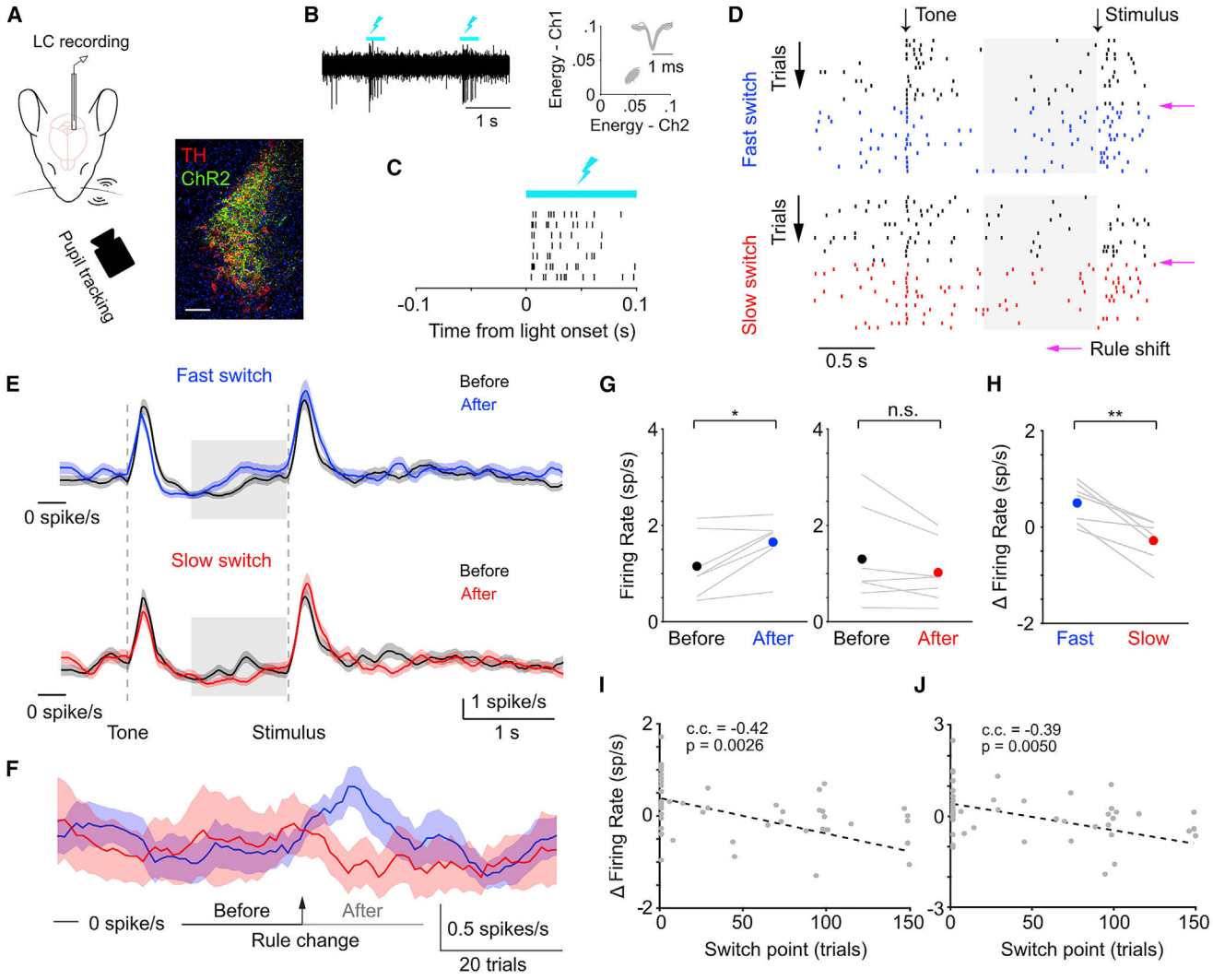

Figure 2. Correlating LC activity with flexible task switching

(A) Schematic of experimental setup during behavior (left) and ChR2 expression in a DBH;Ai32 mouse (right; TH, tyrosine hydroxylase). Scale bar, 200 μm.

(B) Responses of an example ChR2-expressing LC neuron to optical stimulation (left, lightning bolts), and spike-sorting diagram and waveforms of the unit (right).

(C) Example spike responses (ticks) to optogenetic stimulation aligned to stimulation onset (5 ms latency). Rows represent trials.

(D) Example spike raster from an LC unit during a behavior session with both a fast (top) and a slow (bottom) switch block. Rows represent individual trials. Magenta arrows indicate the rule shift. Trials in the previous block are in black, and trials in the current block are in blue (fast) or red (slow). Shaded gray areas represent the 1 s time window to quantify baseline activity.

(E) Average PSTH of LC activity (mean ± SEM) from fast (top, n = 7 sessions) and slow (bottom, n = 7 sessions) switches, quantified before (last 20 trials in the previous block, before) and after the rule change (first 20 trials in the new block, after). Shaded gray areas

represent the 1 s time window to quantify baseline activity. One single-unit recording per session. Same data used in (F)–(H).

(F) Baseline LC activity averaged within each trial and concatenated across 100 trials (mean ± SEM) aligned to the rule change (arrow) for fast (blue) and slow (red) switches. Horizontal bars indicate before and after trial periods to compare baseline LC activity in (G)–(J).

(G) Baseline LC activity during the before and after periods for fast (left, before versus after: 1.15 ± 0.25 versus 1.65 ± 0.19 spikes/s, $p = 0.021$, $t = -3.1$, $n = 7$ sessions) and slow switches (right, before versus after: 1.30 ± 0.39 versus 1.02 ± 0.24 spikes/s, $p = 0.13$, $t = 1.8$, $n = 7$ sessions, two-tailed t test). One single-unit recording per session.

(H) The changes in baseline activity (Δ firing rate = after − before) was higher during fast switches than slow switches. Fast versus slow: 0.50 ± 0.16 versus −0.28 ± 0.16 spikes/s, $p = 0.0020$, $t = 5.2$, $n = 7$ sessions, two-tailed t test. Lines represent individual paired fast-slow blocks from the same session. Dots represent mean. One single-unit recording per session.

(I) The relationship between behavioral switch point and the changes in baseline LC activity. Gray dots represent individual blocks (49 blocks from 34 sessions). c.c., Pearson correlation coefficient. One single-unit recording per session.

(J) Same as in (I), except that baseline LC activity was quantified in a 0.5 s window prior to whisker stimulation onset instead of 1 s.

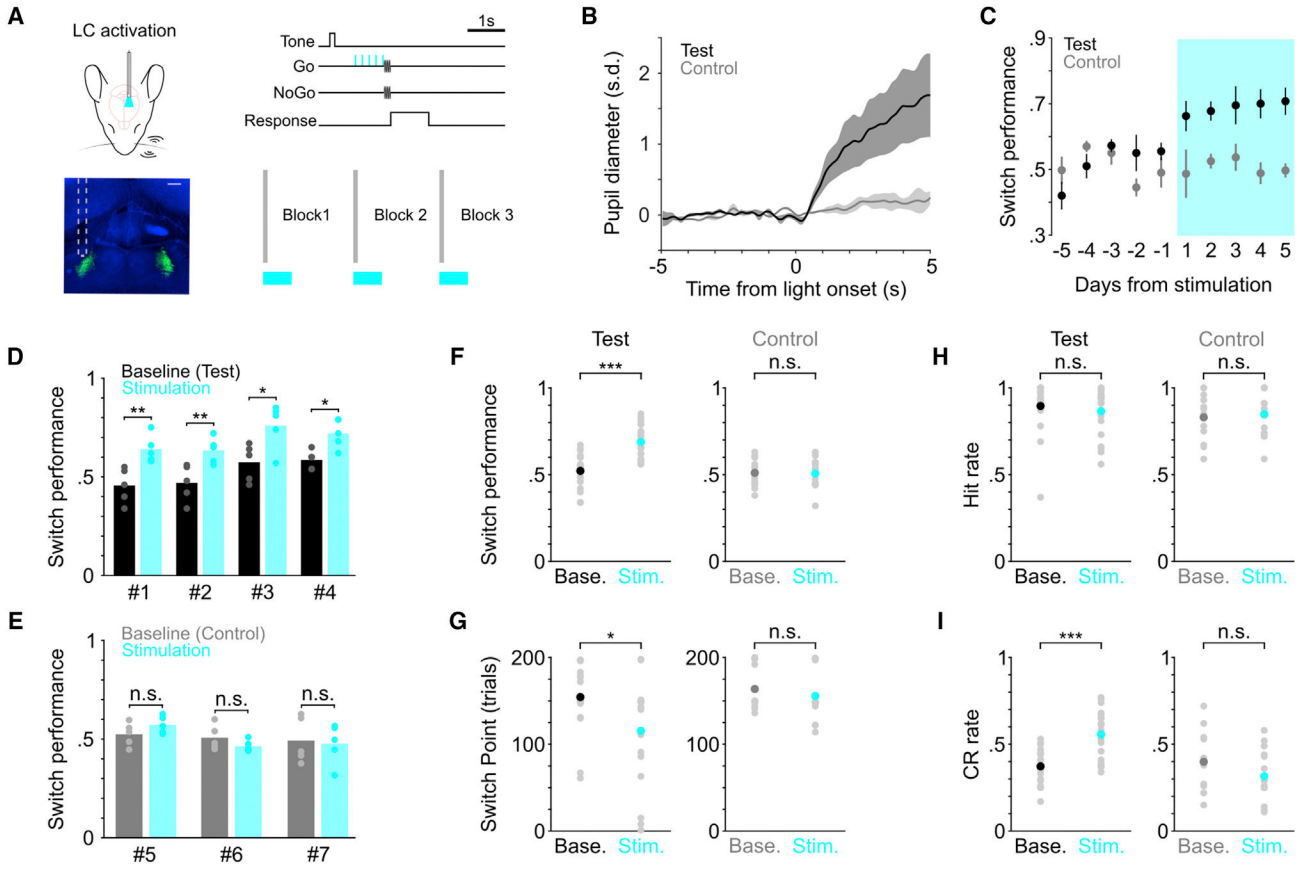

Figure 3. Determining the causal link between LC activity and flexible task switching

(A) Schematic of optogenetic LC stimulation during task performance, and histological section showing the placement of the optical fiber (green, LC). Scale bar, 200 μm.

(B) Group average (mean ± SEM) pupil responses to optical stimulation under anesthesia from the majority of test (black, n = 3) and control (gray, n = 2) mice. Pupil responses from the remaining 1 test mouse and 1 control mouse were quantified in awake behaving condition in Figure S4B.

(C) Group average switch performance for the test (black) and control (gray) groups during baseline (5 consecutive days prior to stimulation) and optical stimulation (5 consecutive days with stimulation, cyan) sessions. Day −1 represents the last day without stimulation. Day 1 represents the first day with stimulation.

(D) Switch performance for individual mice in the test group (n = 4), compared between baseline (black) and stimulation sessions (cyan). Baseline versus stimulation, mouse #1: 0.46 ± 0.04 versus 0.64 ± 0.03, p = 0.008; mouse #2: 0.47 ± 0.04 versus 0.63 ± 0.03, p = 0.004; mouse #3: 0.57 ± 0.04 versus 0.76 ± 0.05, p = 0.012; mouse #4: 0.59 ± 0.02 versus 0.72 ± 0.03, p = 0.024. Permutation test.

(E) Switch performance for individual mice in the control group (n = 3), compared between baseline (gray) and stimulation sessions (cyan). Baseline versus stimulation, mouse #5: 0.53 ± 0.03 versus 0.58 ± 0.01, p = 0.18; mouse #6: 0.51 ± 0.03 versus 0.46 ± 0.02, p = 0.24; mouse #7: 0.50 ± 0.05 versus 0.48 ± 0.05, p = 0.80. Permutation test.

(F) Comparison of switch performance for test (left) and control (right) groups between baseline and stimulation sessions. Baseline versus stimulation, test group: 0.52 ± 0.02 versus 0.69 ± 0.02, p = 1.6e-5, rank sum = 250, n = 20; control group: 0.51 ± 0.02 versus 0.51 ± 0.02, p = 1.0, rank sum = 232, n = 15, two-tailed Wilcoxon rank-sum test. Each mouse contributed 5 consecutive sessions in each condition. Black, dark gray and cyan dots represent mean. Comparisons across mice between test and control groups are shown in Figure S4H.

(G) Comparison of behavioral switch point for test (left) and control (right) groups between baseline and stimulation sessions. Baseline versus stimulation, test group: 154 ± 8 versus 116 ± 13 trials, p = 0.02, rank sum = 495, n = 20; control group: 164 ± 7 versus 156 ± 8 trials, p = 0.23, rank sum = 262, n = 15, two-tailed Wilcoxon rank-sum test. Black, dark gray and cyan dots represent mean. Comparisons across mice between test and control groups are shown in Figure S4H.

(H) Comparison of hit rate for test (left) and control (right) groups between baseline and stimulation sessions. Baseline versus stimulation, test group: 0.90 ± 0.03 versus 0.87 ± 0.03, p = 0.56, rank sum = 432, n = 20; control group: 0.83 ± 0.03 versus 0.85 ± 0.04, p = 0.79, rank sum = 162, n = 15, two-tailed Wilcoxon rank-sum test. Black, dark gray and cyan dots represent mean.

(I) Comparison of correct rejection rate for test (left) and control (right) groups between baseline and stimulation sessions. Baseline versus stimulation, test group: 0.37 ± 0.02 versus 0.56 ± 0.03, p = 2.4e-4, rank sum = 274, n = 20; control group: 0.40 ± 0.04 versus 0.32 ± 0.04, p = 0.15, rank sum = 268, n = 15, two-tailed Wilcoxon rank-sum test. Black, dark gray, and cyan dots represent mean.

KEY RESOURCES TABLE

REAGENT or RESOURCE	SOURCE	IDENTIFIER
Antibodies		
anti-Tyrosine Hydroxylase primary	Thermo Fisher	Cat#OPA1-04050; RRID: AB_325653
anti-Tyrosine Hydroxylase secondary	Thermo Fisher	Cat#A11012; RRID: AB_2534079
anti-EGFP	Thermo Fisher	Cat#A-11039; RRID: AB_25344096
Chemicals, peptides, and recombinant proteins		
Paraformaldehyde	Sigma-Aldrich	Cat#P6148
Experimental models: Organisms/strains		
Mouse: DBH-Cre	MMRRC	RRID: MMRRC_036778-UCD
Mouse: Ai32	JAX	RRID: IMSR_JAX: 024109
Software and algorithms		
MATLAB	Mathworks	https://www.mathworks.com/products/matlab.html
WaveSurfer	HHMI Janelia	https://www.janelia.org/open-science/wavesurfer
DeepLabCut	Mathis et al., 2018	http://www.mackenziemathislab.org/deeplabcut
MClust	Redish, 2014	https://redishlab.umn.edu/mclust
Custom analysis code	This paper	https://doi.org/10.5281/zenodo.7117206
Other		
Tetrode drive	Cohen et al., 2012	N/A
Camera	Basler	#106752
Diode laser	UltraLasers	# MDL-III-450-200mW